Nonvolatile control of transport and magnetic properties in magnetoelectric heterostructures by electric field*

Qian Li(李潜), Dun-Hui Wang(王敦辉)†, Qing-Qi Cao(曹庆琪), and You-Wei Du(都有为)

National Laboratory of Solid State Microstructures and Jiangsu Key Laboratory for Nano Technology, Nanjing University, Nanjing 210093, *China*

(Received 26 April 2017; revised manuscript received 15 May 2017; published online 31 July 2017)

Nonvolatile manipulation of transport and magnetic properties by external electric field is significant for information storage. In this study, we investigate the electric field control of resistance and magnetization in a magnetoelectric heterostructure comprising an electronic phase-separated $La_{0.325}Pr_{0.3}Ca_{0.375}MnO_3$ (LPCMO) thin film and a ferroelectric (011)-oriented $0.7Pb(Mg_{1/3}Nb_{2/3})O_3$-$0.3PbTiO_3$ (PMN-PT) substrate. In a room-temperature poled sample, the metal-to-insulator transition temperature of an LPCMO film increases and the resistance decreases with variation in the effect of the remnant strain. Meanwhile, the increase in the magnetization of the sample is observed as well. This effect would be beneficial for the development of novel storage devices with low power consumption.

Keywords: magnetoelectric heterostructure, electronic phase separation, perovskite manganite, magnetoelectric coupling

PACS: 75.47.Gk, 77.55.Nv, 71.30.+h, 64.75.St **DOI:** 10.1088/1674-1056/26/9/097502

1. Introduction

The electric-field control of transport and magnetic properties in single-phase multiferroics and magnetoelectric (ME) composites has attracted considerable attention for its promising application in information storage and spintronic devices.[1–3] Artificial composites combined ferroelectric (FE) and ferromagnetic (FM) is an excellent candidate for large ME coupling, which is typically achieved by strain or stress coupling at the interface.[4,5] Advancements in high-quality thin film fabrication have enabled the development of FM or other strongly correlated complex oxide layers on FE substrates. In these heterostructures, the electronic or magnetic phases of the films can be effectively tailored by applying an electric field to the FE substrates, thereby leading to a variation in transport or magnetic properties. Various oxides, such as manganites,[6–11] ferrites,[12–14] Mott-insulators,[15] and dilute magnetic semiconductors,[16] were integrated in such heterostructures, and therefore strain-mediated electric field control effects were observed.

A typically strong correlated complex oxide, that is, electronic phase-separated (EPS) manganite, in which ferromagnetic metallic (FMM) phase and charge-ordered insulating (COI) phase coexist and distribute inhomogeneously owing to strong spin–charge–lattice coupling, is of particular interest for the discoveries of the first-order metal-to-insulator transition (MIT) and other fascinating emergent phenomena under external conditions such as spatial confinement.[17,18] Owing to the self-organized "electronically soft" nature, the phase domains in an EPS thin film are dramatically affected by the in-plane strain.[19,20] For example, the prototype EPS manganite $La_{5/8-x}Pr_xCa_{3/8}MnO_3$ ($x = 0.3$) deposited on an orthorhombic $NdGaO_3$ substrate exhibits remarkable in-plane anisotropic transport behavior, while the relative difference of mismatch between the two in-plane directions is only $\sim 1.3\%$.[20] Thus, the modulation of EPS manganites in strain-mediated ME heterostructures is expected to be considerable. Recently, electric field induced or tailored phenomena in EPS manganites/FE heterostructures, such as large electroresistance,[21] abnormal percolative transport,[22,23] and modulation of persistent photoconductivity[24] or photoinduced effect,[25] were reported, demonstrating that the coexistence of different electronic phases can be modulated by electric field. Nevertheless, linear-converse piezoelectric response of FE crystal was used for inducing changes in the magnetic anisotropy and distribution of different phases in previous studies, so that a relatively large electric field (8–10 kV/cm) applied *in situ* is necessary for maintaining these changes, which will vanish once the field is removed. From the point of view of information storage, it is still worth exploring the nonvolatile control of transport and magnetic properties in the EPS manganite by electric field.

The perovskite $(1\text{-}x)Pb(Mg_{2/3}Nb_{1/3})O_3 - xPbTiO_3$ ($x \approx 0.3$) (PMN-PT) single crystal is one of the most widely used FE substrates owing to its high performance of ferroelectric and piezoelectric activities.[26] In PMN-PT-based ME heterostructures, both volatile and nonvolatile electric field control effects are reported, depending on the special substrate orientation and the approach of the application of an elec-

*Project supported by the National Natural Science Foundation of China (Grant No. 51571108).

†Corresponding author. E-mail: wangdh@nju.edu.cn

© 2017 Chinese Physical Society and IOP Publishing Ltd

tric field. Particularly, in a (011)-oriented PMN-PT single crystal, two distinct, nonvolatile and reversible remnant in-plane strain states can be achieved by applying an electric field with appropriate magnitude (less than the coercive field of FE layer).[27,28] Recently, nonvolatile control of transport and magnetic properties induced by the electric field controllable remnant strain states was observed in several ME heterostructures.[10,11,14,15] Therefore, a natural consideration is that the combination of the special remnant strain states and the EPS manganites can achieve the nonvolatile electric field control of the transport and magnetic properties simultaneously, because they belong to strongly correlated electronic systems and their physical properties are sensitive to the external strain.

In this study, a $La_{5/8-x}Pr_xCa_{3/8}MnO_3$ ($x = 0.3$) film, which is reported as the ideal model system of an EPS manganite with a large-scale phase coexistence, is epitaxially deposited on PMN-PT (011) substrate to form a ME heterostructure. The transport and magnetic properties under different poled states are investigated. When the heterostructure is poled by a low electric field (less than 1.5 kV/cm), both the resistivity and magnetization of the LPCMO film are remarkably modulated in a wide temperature region as a result of the nonvolatile remnant in-plane strain of the PMN-PT substrate.

2. Experimental

The $La_{0.325}Pr_{0.3}Ca_{0.375}MnO_3$ (LPCMO) film with the thickness of $\sim$ 120 nm was epitaxially deposited on a (011)-oriented PMN-PT single crystal substrate by pulsed laser deposition (PLD) using a KrF excimer laser with a wavelength of 248 nm. During growth, the grown temperature and oxygen pressure were fixed at 700 °C and 90 Pa, respectively. The laser energy density was fixed at 2 J/cm^2 and the repetition rate was 5 Hz. After deposition, the LPCMO film was annealed *in situ* for 30 min, and then slowly cooled to room temperature under the same oxygen pressure used during growth. Structural characterization of the heterostructure was conducted using an x-ray diffractometer (XRD) at room temperature using Cu $K_{\alpha 1}$ radiation ($\lambda = 1.54056$ Å). The electrical transport measurements were performed using the four-probe method in a closed cycle helium cryostat, in which the temperature can be controlled between 10 K and room temperature with an accuracy of better than 0.05 K. The in-plane resistance of the LPCMO film was obtained using a Keithley 6220 current source and a Keithley 2182A nanovoltmeter. The electric field was applied along the thickness direction of the PMN-PT substrate using a Keithley 2410 source meter. A 100 nm-thick Au film is sputtered on the backside of the substrate as the bottom electrode, and the in-plane strain of the sample is measured using a strain gauge bonded on the LPCMO film. The magnetic properties were measured using a superconducting quantum interference devices magnetometer (SQUID, Quantum Design).

3. Results and discussion

The characterization of the strain states under different poling electric fields is essential for understanding the electric field control effect. Figure 1(a) shows the in-plane strain as a function of the asymmetric bipolar electric field (S–E) with different maximum positive amplitudes along the in-plane [100] directions of the PMN-PT (011) single crystal, respectively. The coercive field of this substrate is determined to be approximately 1.6 kV/cm by the S–E loop under the symmetric unipolar electric field with a maximum amplitude of 8 kV/cm (not shown). In the rhombohedral phase of the PMN-PT single crystal, the spontaneous ferroelectric polarization directions are along its eight $\langle 111 \rangle_c$ orientations.[17] For (011)-oriented PMN-PT crystal, four of them are in-plane and others are out-of-plane. For the negative poled crystal, the out-of-plane polarization directions are oriented to the two downward directions (see Fig. 1(b)).[14,27] When an asymmetric bipolar electric field is swept from zero to 1.5 kV/cm on the negatively poled substrate, 71°/109° domain switching occurs with the polarization directions changing to four possible in-plane directions (see Fig. 1(c)), thereby leading to a significant in-plane strain that can remain if the electric field returns back to zero, as shown in Fig. 1(a).[14,27] Afterwards, when an electric field of -8 kV/cm is applied, the polarization rotates back to the downward directions, and the strain recovers to its initial state once the electric field is removed. As a result, a hysteresis-like S–E loop with remnant strain states c and a can be observed. Moreover, when the maximum positive electric field amplitude is adjusted to 1.3 kV/cm, a minor S–E loop with a smaller remnant strain state b can be obtained, thereby indicating that the value of remnant strain can be manipulated by applying an appropriate electric field to the PMN-PT (011) substrate.

The XRD pattern for the LPCMO/PMN-PT (011) heterostructure is shown in Fig. 2, where the out-of-plane reflections corresponding to the (011) orientation can be observed, thereby indicating a single-phase and highly oriented nature of the film. The out-of-plane lattice constant of the LPCMO film calculated from these (011) diffraction peaks is determined to be $d_{\text{film}} \approx 2.69$ Å, which is smaller than that of the bulk value ($d_{\text{bulk}} \approx 2.71$ Å). The out-of-plane strain (ε_{zz}) can be estimated as -0.72% using $\varepsilon_{zz} = (d_{\text{film}} - d_{\text{bulk}})/d_{\text{bulk}}$, thereby indicating that the LPCMO film on PMN-PT substrate experiences a compressive strain along the out-of-plane direction. Meanwhile, the corresponding average in-plane tensile strain (ε_{xx}) can be calculated as 0.61% by using the Poisson relation $\varepsilon_{xx} = ((1-\nu)/2\nu)\varepsilon_{zz}$ (ν is the Poisson ratio), in which $\nu = 0.372$, calculated in a similar compound

$(La_{2/3}Pr_{1/3})_{0.625}Ca_{0.375}MnO_3$,[29] is selected. The inset of Fig. 2 presents the schematic of the device for in-plane resistance measurements. Poling PMN-PT is achieved through applying an electric field in the thickness direction, using the LPCMO and a sputtered Au film as top and bottom electrodes, respectively. An electric field of −8 kV/cm is applied to the heterostructure for 10 min at room temperature before each measurement of transport and magnetic properties to ensure that the polarization vector is pointing downward.

The temperature dependences of resistivity (ρ–T) for the LPCMO layer along the in-plane [100] direction under different poled states are shown in Fig. 3. In the unpoled state a, the ρ–T curves for both in-plane directions exhibit first-order MIT with obvious thermal hysteresis. Upon cooling, the transition from insulator to metal happens at $T_{C1} \approx 92$ K, while the metal-to-insulator transition happens at $T_{C2} \approx 98$ K during the warming process. At room temperature, a poling electric field of 1.3 kV/cm is applied on the PMN-PT substrate and then removed. This leads to the remnant strain of state b in Fig. 1(a). Then, the ρ–T curve changes evidently. As shown in Fig. 3, the increase of MIT temperature and decrease of resistivity can be observed, thereby suggesting that the nucleation, growth, and maintenance of FMM domains are easier in the poled heterostructure. Such a variation is more remarkable when a larger poling electric field of 1.5 kV/cm is applied, which is attributed to the larger remnant strain of state c. The relative difference in resistivities at MIT temperatures (92 K and 96 K for state a and c, respectively) upon cooling $((\rho(\mathrm{MIT,c})–\rho(\mathrm{MIT,a}))/\rho(\mathrm{MIT,a}))$ can be calculated as −18.4%. It is worth noting that the electric field is not applied *in situ* during the measurement. Therefore, the nonvolatile control of the transport properties is achieved.

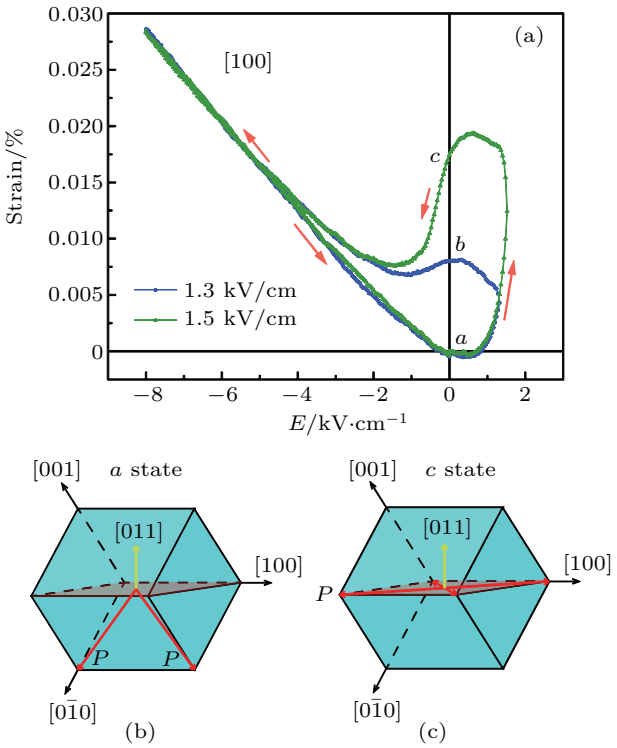


Fig. 1. (color online) (a) In-plane strain of PMN-PT (011) substrate along [100] directions as a function of asymmetric bipolar electric field (S–E) with different maximum positive amplitudes. (b) and (c) illustrate the directions of ferroelectric polarization states in remnant strain states *a* and *c*, respectively.

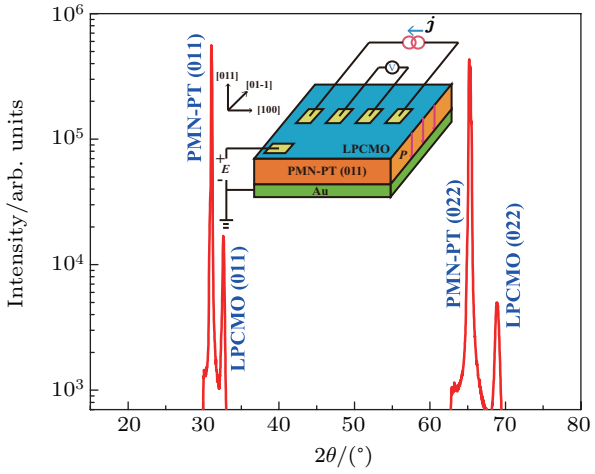


Fig. 2. (color online) X-ray diffraction pattern for LPCMO/PMN-PT (011) heterostructure. Inset: schematic of the heterostructure for anisotropic in-plane resistance measurements.

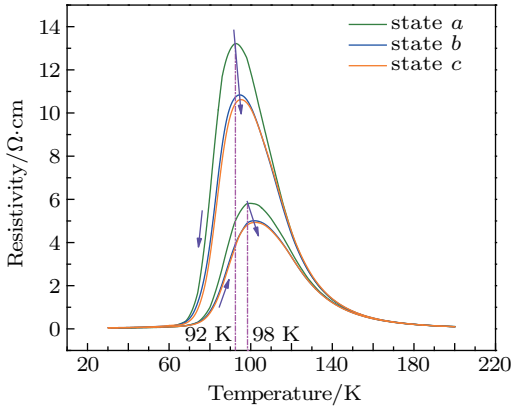


Fig. 3. (color online) Temperature dependences of resistivity (ρ–T) for LPCMO layer along in-plane [100] direction under different poled states.

Figure 4 shows the temperature dependences of magnetization (M–T) for the LPCMO/PMN-PT (011) heterostructure under different poled states. The magnetic field is fixed at 200 Oe during the measurement and is parallel to the in-plane [100] direction. For state a, a thermal hysteresis can be observed in the M–T curve, indicating that the transition between the FMM phase and the COI phase in LPCMO is a first-order transition, which is consistent with the result of the transport measurement. After a poling electric field of 1.5 kV/cm is applied at room temperature and then removed (state c), the increase of the magnetization can be observed. The relative changes of magnetization ($\Delta M = (M(\mathrm{c}) - M(\mathrm{a}))/M(\mathrm{a})$) are 2.19% and 2.37% at 10 K and 90 K (upon cooling), respectively. Meanwhile, a slight increase in the ferromagnetic Curie

temperature is observed, suggesting that the exchange interaction of the FMM phase is also enhanced.

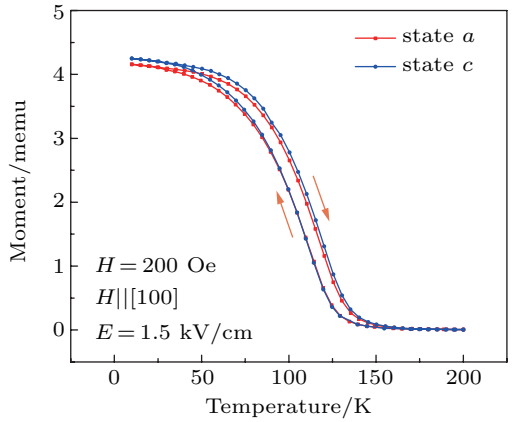


Fig. 4. (color online) Temperature dependences of magnetic moment (M–T) for LPCMO/PMN-PT (011) heterostructure under different poled states.

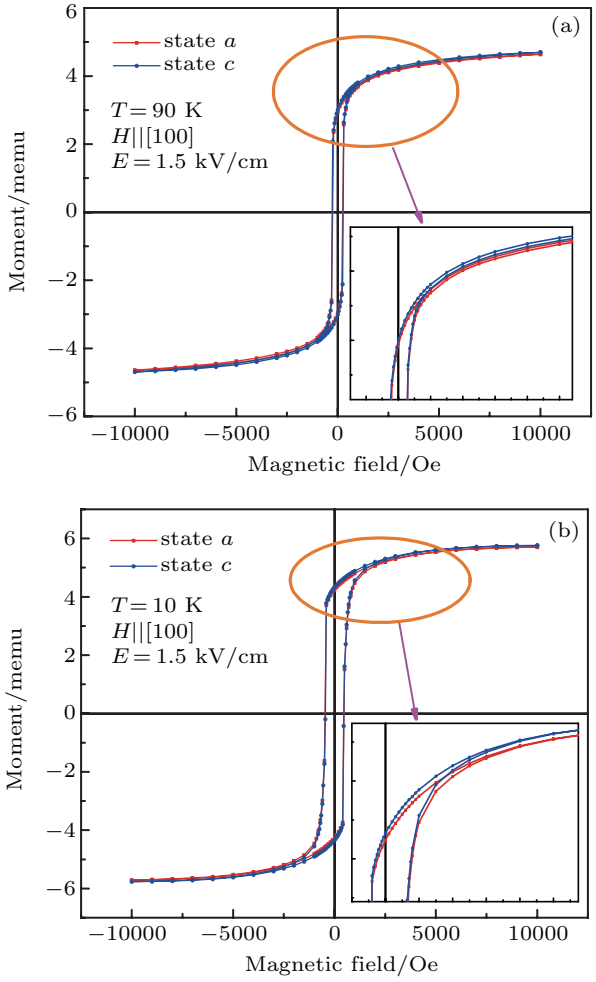


Fig. 5. (color online) Magnetic hysteresis (M–H) loops upon cooling under different poled states for (a) $T = 90$ K, $\boldsymbol{H} \parallel [100]$, and (b) $T = 10$ K, $\boldsymbol{H} \parallel [100]$. The inset shows local enlargement of M–T curves in a selected region.

To further demonstrate the nonvolatile magnetization change by electric field, the magnetic hysteresis (M–H) loops upon cooling under different poled states at some special temperatures are investigated. As shown in Fig. 5(a) and 5(b), the M–H loops are measured at $T = 90$ K and $T = 10$ K, respectively, while the magnetic field is applied along the in-plane [100] directions. For $T = 90$ K, the LPCMO layer is in the hysteresis region, that is, the two phases coexisting region, and exhibits a ferromagnetic-like M–H loop. After poling by an electric field of 1.5 kV/cm, the high-field magnetization increases. For $T = 10$ K, the LPCMO film is almost dominated by the FMM phase, in which an M–H loop with a larger magnetic moment is observed. In this case, a similar but more obvious variation of high-field magnetization is observed.

In the study of FM/FE ME heterostructures, the electric field control of FM layers is typically ascribed to the coaction of electric-field-induced strain and polarization charge effects.[7] Nevertheless, PMN-PT (011) single crystal shows a ferroelectric $\boldsymbol{D}$–$\boldsymbol{E}$ loop (electric displacement $\boldsymbol{D}$ as a function of applied electric field $\boldsymbol{E}$) with large saturation and remnant polarization only when the maximum applied electric field is greater than its coercive field. Otherwise, a linear but small electric displacement is exhibited.[27] In our experiments, the remnant polarization of the substrate is neglectable because the poling electric field is less than the coercive field. Therefore, we conclude that the nonvolatile control of an LPCMO film can be ascribed to the electric-field-induced remnant strain.

As previously mentioned, the LPCMO film experiences an in-plane tensile strain in the heterostructure. Moreover, the remnant strain under an asymmetric bipolar electric field is positive, thereby indicating an enhanced tensile strain in the poled sample. Accurately, the influence of an epitaxial tensile strain on the transport properties in an EPS manganite originates from two aspects as follows.[22] First, the tensile strain can act as a driving force in the nucleation and growth of FMM domains owing to the fact that a large-scale EPS can self-organize into elongated domains along the direction with a stronger tensile strain.[20] As a result, the formation of percolative channel is facilitated in the poled sample, which is primarily responsible for the increase of MIT temperature and the decrease of resistivity. Second, the anisotropic in-plane strain field typically leads to the distortion of the in-plane MnO_6 octahedron in manganite, and therefore affects the occupation of the 3d orbitals of the Mn ion, thereby resulting in the suppression of the long-range charge or orbital ordering state.[21] Thus, the volume fraction of the FMM phase in the LPCMO film may increase and the enhanced ferromagnetism is shown. However, both aspects exhibit little effect on the exchange interaction of FMM domains, so that the variation in ferromagnetic Curie temperature is not remarkable.

4. Summary

In this study, we investigated a nonvolatile electric field control of the transport and magnetic properties in an ME LPCMO/PMN-PT (011) heterostructure. In this heterostructure, the LPCMO film shows a first-order MIT. When a relatively small electric field (less than its ferroelectric coercive field) is applied at room temperature, the MIT temperature of the LPCMO layer increases and the resistance in its thermal hysteresis region decreases with variation in the effect of the remnant stain. Meanwhile, the magnetization of the sample is increased. In other words, the nonvolatile manipulation of the transport and magnetic properties by electric field is achieved. This effect can be ascribed to the modulation of the percolative transport and the suppression of the long-range charge or orbital ordering state that is induced by the remnant strain, and it may be helpful for the development of novel storage devices with low power consumption.

References

[1] Spaldin N A and Fiebig M 2005 *Science* **309** 391
[2] Eerenstein W, Mathur N D and Scott J F 2006 *Nature* **442** 759
[3] Martin L W, Crane S P, Chu Y H, Holcomb M B, Gajek M, Huijben M, Yang C H, Balke N and Ramesh R 2008 *J Phys.: Condens. Matter* **20** 434220
[4] Wang Y, Hu J, Lin Y and Nan C W 2010 *NPG Asia Mater.* **2** 61
[5] Vaz C A F, Hofman J, Ahn C H and Ramesh R 2010 *Adv. Mater.* **22** 2900
[6] Tiele C, Dörr K, Bilani O, Rödel J and Schultz L 2007 *Phys. Rev. B* **75** 054408
[7] Sheng Z G, Gao J and Sun Y P 2009 *Phys. Rev. B* **79** 174437
[8] Chen Q P, Yang J J, Zhao Y G, Zhang S, Wang J W, Zhu M H, Yu Y, Zhang X Z, Wang Z, Yang B, Xie D and Ren T L 2011 *Appl. Phys. Lett.* **98** 172507
[9] Yang Y, Luo Z L, Yang M M, Huang H, Wang H, Bao J, Pan G, Gao C, Hao Q, Wang S, Jokubaitis M, Zhang W, Xiao G, Yao Y, Liu Y and Li X G 2013 *Appl. Phys. Lett.* **102** 033501
[10] Zhao W, Zhang D, Meng D, Huang W, Feng L, Hou C, Lu Y, Yin Y and Li X 2016 *Appl. Phys. Lett.* **109** 263502
[11] Zhou W, Xiong Y, Zhang Z, Wang D, Tan W, Cao Q, Qian Z and Du Y 2016 *ACS Appl. Mater. Interfaces* **8** 5424
[12] Yang J J, Zhao Y G, Tian H F, Luo L B, Zhang H Y, He Y J and Luo H S 2009 *Appl. Phys. Lett.* **94** 212504
[13] Park J H, Jeong Y K, Ryu S, Son J Y and Jang H M 2010 *Appl. Phys. Lett.* **96** 192504
[14] Liu M, Hofman J, Wang J, Zhang J, Nelson-Cheeseman B and Bhattacharya A 2013 *Sci. Rep.* **3** 1876
[15] Nan T, Liu M, Ren W, Ye Z G and Sun N X 2014 *Sci. Rep.* **4** 5931
[16] Zhu Q X, Yang M M, Zheng M, Zheng R K, Guo L J, Wang Y, Zhang J X, Li X M, Luo H S and Li X G 2015 *Adv. Func. Mater.* **25** 1111
[17] Dagotto E, Hotta T and Moreo A 2001 *Phys. Rep.* **344** 1
[18] Shen J, Ward T Z and Yin L F 2013 *Chin. Phys. B* **22** 017501
[19] Ahn K H, Lookman T and Bishop A R 2004 *Nature* **428** 401
[20] Ward T Z, Budai J D, Gai Z, Tischler J Z, Yin L and Shen J 2009 *Nat. Phys.* **5** 885
[21] Zheng M, Li X Y, Yang M M, Zhu Q X, Wang Y, Li X M, Shi X, Chan H L W, Li X G, Luo H S and Zheng R K 2013 *Appl. Phys. Lett.* **103** 263507
[22] Zhao Y Y, Wang J, Kuang H, Hu F X, Zhang H R, Liu Y, Zhang Y, Wang S H, Wu R R, Zhang M, Bao L F, Sun J R and Shen B G 2014 *Sci. Rep.* **4** 7075
[23] Jiang T, Wang X, Shen C, Wang X, Peng L, Fan L and Wu W 2016 *Appl. Phys. Lett.* **108** 113504
[24] Wang J F, Jiang Y C, Wu Z P and Gao J 2013 *Appl. Phys. Lett.* **102** 071913
[25] Li W, Dong X L, Wang S H and Jin K X 2016 *Appl. Phys. Lett.* **109** 091907
[26] Noheda B, Cox D E, Shirane G, Gao J and Ye Z G 2002 *Phys. Rev. B* **66** 054104
[27] Wu T, Zhao P, Bao M, Bur A, Hockel J L, Wong K, Mohanchandra K P, Lynch C S and Carman G P 2011 *J. Appl. Phys.* **109** 124101
[28] Wu T, Bur A, Wong K, Zhao P, Lynch C S, Amiri P K, Wang K L and Carman G P 2011 *Appl. Phys. Lett.* **98** 262504
[29] Zhu Y, Du K, Niu J, Lin L, Wei W, Liu H, Lin H, Zhang K, Yang T, Kou Y, Shao J, Gao X, Xu X, Wu X, Dong S, Yin L and Shen J 2016 *Nat. Commun.* **7** 11260